ON THE VARIATIONS IN THE INSOLATION AT MERCURY RESULTING FROM OSCILLATIONS OF THE ORBITAL ECCENTRICITY

E. VAN HEMELRIJCK
Belgian Institute for Space Aeronomy, Brussels, Belgium

(Received 14 June, 1983)

Abstract. This paper describes variations in the insolation on Mercury resulting from fluctuations of the orbital eccentricity ($0.11 \leqslant e \leqslant 0.24$) of the planet. Equations for the instantaneous and the daily insolation are briefly discussed and several numerical examples are given illustrating the sensitivity of the solar radiation to changes in e. Special attention is paid to the behavior of the solar radiation distribution curves near sunrise and sunset which at the warm pole of Mercury (longitudes $\pm 90°$) occur as the planet goes through perihelion. It has been found that for eccentricities larger than about 0.194 there exists two permanent thermal bulges on opposite sides of the Mercurian surface that alternately point to the Sun at every perihelion passage. The critical value of e past which the Sun shortly sets after perihelion is near 0.213.

1. Introduction

Since the work of Brouwer and van Woerkom (1950) on the theory of secular variations of the planetary elements, it has been possible to calculate the long-term periodic oscillation of the orbital eccentricity of Mercury caused by gravitational perturbations from the Sun and the other planets. Now, we know (Cohen *et al.*, 1973; Ward *et al.*, 1976; Van Flandern and Harrington, 1976) that the eccentricity e of Mercury is currently 0.205 63, whereas it ranges from a value near 0.11 to a theoretical maximum of approximately 0.24 during the dynamical history of the planet. The oscillation has two superposed periods: one of 10^5 yr and another of 10^6 yr.

Some aspects of the solar radiation incident at the top of the atmosphere of Mercury have been studied by e.g. Soter and Ulrichs (1967), Liu (1968), Vorob'yev and Monin (1975), Van Hemelrijck and Vercheval (1981) and Landau (1982). In their computations the above mentioned authors used the present value of the eccentricity. However, the solar radiation being strongly dependent upon this parameter, it is obvious that important periodic insolation variations on Mercury are closely associated with fluctuations in e. In this paper, therefore, we will study the effect of the time evolution of the eccentricity on the insolation at Mercury.

In a first section, we briefly discuss some formulas needed for the computation of the insolation. For more details on solar radiation investigation we refer to Ward (1974), Vorob'yev and Monin (1975), Levine *et al.* (1977), Van Hemelrijck and Vercheval (1981, 1983), Landau (1982) and Van Hemelrijck (1982a, b, c, d; 1983a, b). Then, the influence of the oscillating orbital eccentricity on the instantaneous as well as on the daily upper-boundary insolation is presented.

The Moon and the Planets **29** (1983) 83–93. 0165-0807/83/0291-0083$01.65.

2. Calculation of the Insolation

The instantaneous insolation (I) is defined as the solar heat flux sensed at a given time by a horizontal unit area of the top of the atmosphere at a given point and per unit time.

Assuming the Sun as a point source I we may write

$$\begin{aligned} I &= (S_0/r_\odot^2)\cos z \quad \text{if} \quad z < \pi/2, \\ I &= 0 \qquad\qquad\quad \text{if} \quad z \geqslant \pi/2, \end{aligned} \tag{1}$$

with

$$r_\odot = a_\odot(1-e^2)/(1+e\cos W); \tag{2}$$

and, for Mercury (Van Hemelrijck and Vercheval, 1981)

$$z = \Delta\lambda + nt - W, \tag{3}$$

where S_0 is the solar constant at the mean Sun–Earth distance of 1 AU taken at 1.96 cal $cm^{-2}(min)^{-1}$ or 2.82×10^3 cal cm^{-2}(planetary day)$^{-1}$ (Wilson, 1982), $r_\odot$ is the heliocentric distance, $a_\odot$(0.3871 AU) is the semi-major axis, e is the eccentricity, W is the true anomaly, z is the zenith angle of the center of the sun, $\Delta\lambda$ is the longitude difference between the meridian of the surface element considered and the meridian crossing the line of apsides at the perihelion passage of the planet which is taken as $t = 0$ and n (6.138 11) is the rotational angular velocity of the planet. Furthermore, keeping only terms up to the third degree in e (which is sufficiently accurate for our calculations), the true anomaly W is given by

$$\begin{aligned} W = {} & n_0 t + (2e - e^3/4)\sin n_0 t + (5/4)e^2 \sin 2n_0 t + \\ & + (13/12)e^3 \sin 3n_0 t, \end{aligned} \tag{4}$$

where n_0 (4.092 35) designates the mean angular motion.

As already pointed out by Landau (1975, 1982) a problem arises near sunrise and sunset when the horizon intersects the Sun's disk. This is particularly true at longitudes $\Delta\lambda = \pm 90^\circ$ where e.g. for the current value of the eccentricity the Sun takes approximately 18 days to rise or set. Indeed, for $z > \pi/2$ some parts of the Sun may still be above the horizon and the instantaneous insolation will be different from zero. For $z < \pi/2$ the centroid of the visible portion of the Sun's disk will be smaller than z and I will again be greater than the insolation obtained by expression (1).

If we take into account the finite angular size of the solar disk at the intersection by the horizon, the instantaneous insolation I is, in a very good approximation, given (cf. Landau 1975, 1982) by

$$I = (S_0/r_\odot^2) f \cos z', \tag{5}$$

with

$$f = 1/2 + (u + \sin u \cos u)/\pi, \tag{6}$$

$$z' = z - 2R\cos^3 u/3\pi f; \tag{7}$$

where f is the fractional area of the Sun above the horizon, z' is the zenith angle of the centroid of this area and R is the angular radius of the Sun and depends upon the heliocentric distance $r_\odot$. Finally, the parameter u is defined as

$$u = \arcsin [(\pi/2 - z)/R]. \tag{8}$$

The daily insolation (I_D) can be found by integrating relation (1) or (5) numerically over a period equal to the planet's solar day $T_\odot$ ($\sim$ 176 Earth days)

$$I_D = \int_{t=0}^{T_\odot} I \, dt. \tag{9}$$

Practically, relationship (9) may also be written as

$$I_D = \int_0^{t_1} I \, dt + \int_{t_2}^{T_\odot} I \, dt, \tag{10}$$

where t_1 and t_2 correspond respectively to the time of setting and rising of the Sun [note that I is always positive using formula (10)]. The integration limits (t_1 and t_2) for a specific value of $\Delta\lambda$ may be determined from the following relations (see Van Hemelrijck and Vercheval, 1981)

$$nt_2 - W(t_2) = 270^\circ - \Delta\lambda, \tag{11}$$

and

$$nt_1 - W(t_1) = 90^\circ - \Delta\lambda; \tag{12}$$

and from the graphical representation of the expression $f(t) = nt - W(t)$ as a function of time. The accuracy obtained with this method is sufficiently high considering the small value of the solar radiation in the vicinity of the lower and upper time limits.

3. The Instantaneous Insolation

The distribution of the equatorial instantaneous insolation on the meridians $\Delta\lambda = 0$ (the so-called hot pole) and $\Delta\lambda = -90^\circ$, (warm pole) for three different values of the eccentricity ($e = 0.11$, 0.205 63 and 0.24) is respectively illustrated in Figures 1 and 2. It has to be emphasized that the instantaneous solar radiation at a given time and at a given latitude (φ) can easily be found by multiplying the insolation on the same meridian at the same moment by the correction factor $\cos\varphi$ and for a surface element located on the equator $\varphi = 0$ (Van Hemelrijck and Vercheval, 1981).

From Figure 1 ($\Delta\lambda = 0$), it can be seen that the maximum solar radiation is incident at the first perihelion passage of the planet with values ranging from 3.1×10^4 ($e = 0.24$) to approximately 2.5×10^4 cal cm^{-2} (planetary day)$^{-1}$ ($e = 0.11$), the percent difference of these two maxima being of the order of 25%. Furthermore, from day 10 until sunset (day 44) the difference between the insolation curves for $e = 0.24$ and $e = 0.11$ equals nearly 10%. For exactly half a solar day ($\sim$ 88 Earth days, not visible on Figure 1) or more precisely from the first aphelion passage to the next one, all parts of the

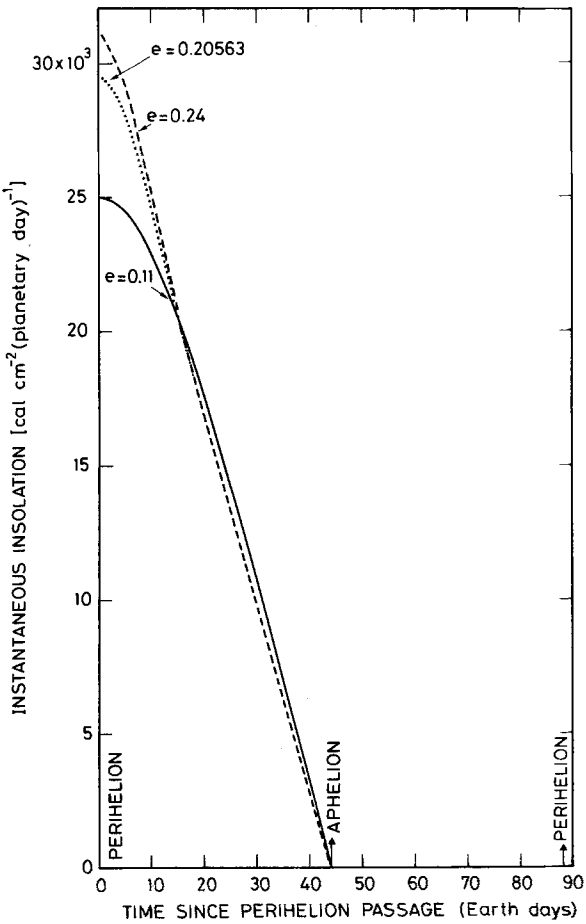

Fig. 1. Time variation of the instantaneous insolation at the top of the Mercurian atmosphere on the meridian $\Delta\lambda = 0°$ and for the following numerical values of the eccentricity e: 0.11, 0.205 63 and 0.24. The curves are related to the equator. Perihelion and aphelion passages are also illustrated.

meridian $\Delta\lambda = 0$ are in permanent darkness. Finally, another maximum is found on the third perihelion passage of Mercury.

In Figure 2 we have plotted the solar radiation incident at the top of the Mercurian atmosphere as a function of time for $\Delta\lambda = -90°$ and for the three eccentricities under consideration. The time evolution of the instantaneous insolation extends, as in Figure 1, over one sidereal period of revolution (or one tropical year). Figure 2 reveals that the insolation distributions are quasi-parallel and that the percentage differences are obviously higher than those obtained for $\Delta\lambda = 0$. The maximum insolation at aphelion amounts to about 1.6×10^4 ($e = 0.11$) and 1.2×10^4 cal cm^{-2} (planetary day)$^{-1}$ ($e = 0.24$) corresponding to a percentage difference of the order of 35%. Before and after aphelion the percent differences are significantly higher.

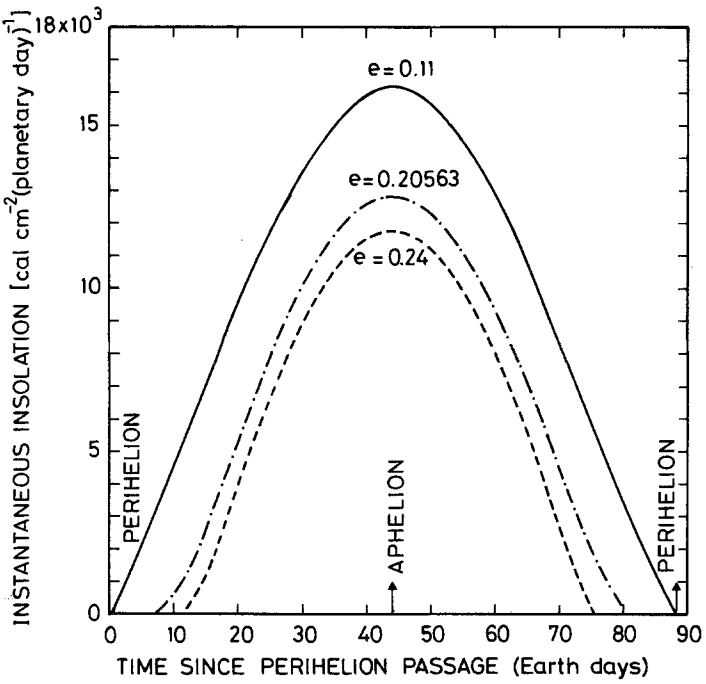

Fig. 2. Time variation of the instantaneous insolation at the top of the Mercurian atmosphere on the meridian $\Delta\lambda = -90°$. See Figure 1 for full explanation.

The insolation curves represented in Figure 2 were computed by assuming the Sun as a point source. However, near sunrise and sunset, which at longitudes $\pm 90°$ occur as Mercury goes through perihelion, more accurate calculations are needed (Landau 1975, 1982) particularly due to the fact that the Sun takes mostly several days to rise or set completely (Landau, 1982; Van Hemelrijck and Vercheval, 1983).

These calculations are given in Figure 3 for the three adopted values of the eccentricity.

From this Figure, it can be seen that the solar radiation distribution slightly before the perihelion passage of the planet results in a thermal bulge (Soter and Ulrichs, 1967; Liu, 1968; Morrison, 1970; Van Hemelrijck and Vercheval, 1981, 1983; Landau, 1982) for eccentricities equal to 0.205 63 and 0.24; for $e = 0.11$ the temporal increase of the upper-boundary solar heat flux does not take place. Furthermore, it is obvious that the shape of the curves is markedly different in passing from the minimum to the maximum value of e.

The reason for the apparition of the thermal bulges at large eccentricities is that, in the neighbourhood of the perihelion, the Mercurian angular velocity of revolution ($\dot{W}$) exceeds the rotational angular velocity (n) of the planet on its own axis. This phenomenon is illustrated in Figure 4, the curves representing the variability of $\dot{W}$ being obtained by Kepler's second law

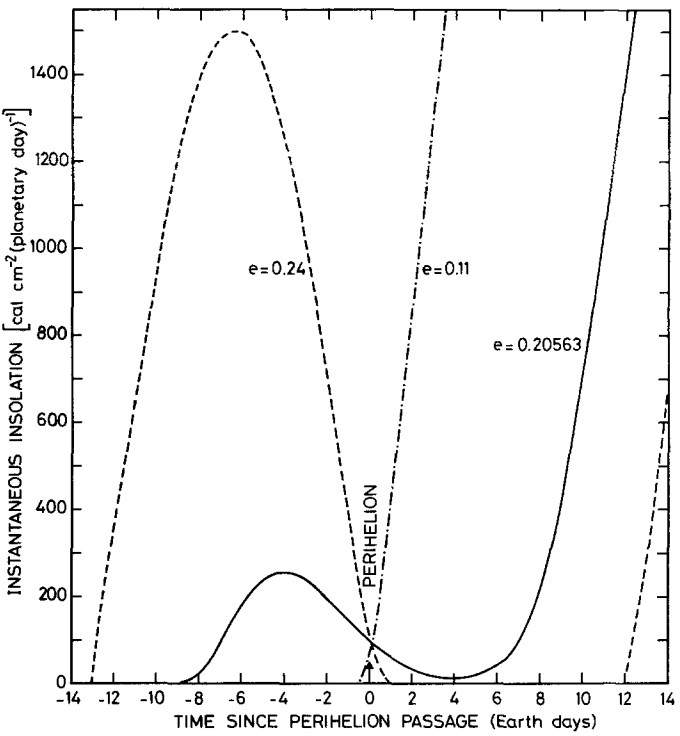

Fig. 3. Time variation of the instantaneous insolation at the top of the Mercurian atmosphere on the warm pole ($\Delta\lambda = -90°$) from 14 days before to 14 days after the perihelion passage.

$$\dot{W} = n_0(1-e^2)^{1/2}(a_\odot/r_\odot)^2, \tag{13}$$

with

$$(a_\odot/r_\odot)^2 = 1 + e^2/2 + (2e + 3/4e^3)\cos M + (5/2)e^2\cos 2M + \\ + (13/4)e^3\cos 3M; \tag{14}$$

where M is the mean anomaly. Note that in expression (14) we kept only terms up to the third degree in e.

Figure 4 clearly demonstrates that $\dot{W} \geqslant n$ from 4 days ($e = 0.205\,63$), respectively 7 days ($e = 0.24$), before to 4 days ($e = 0.205\,63$), respectively 7 days ($e = 0.24$), after the perihelion passage. For the minimum value of the orbital eccentricity ($e = 0.11$), $\dot{W} < n$ over the entire time interval. On the other hand it has been found (Van Hemelrijck and Vercheval, 1983) that the minimum value of e past which $\dot{W} \geqslant n$ is approximately equal to 0.194. In other words, for eccentricities larger than the above mentioned limit, there exist two permanent thermal bulges on opposite sides of the Mercurian surface that alternately point to the Sun at every perihelion passage.

As already stated previously the behavior of the solar radiation distribution curves (Figure 3) for $e = 0.205\,63$ and $e = 0.24$ is fundamentally different. Indeed, for the actual value of e it can be mathematically demonstrated (Turner, 1978; Landau, 1982;

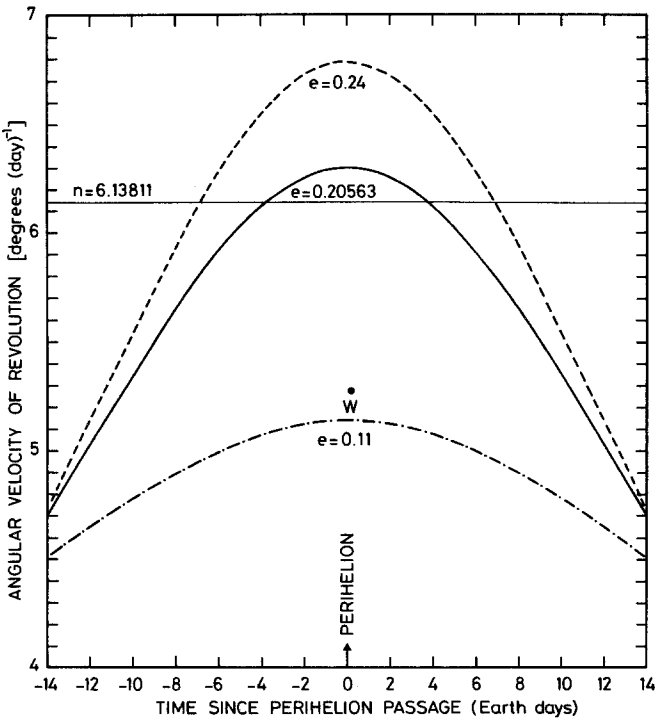

Fig. 4. Mercurian angular velocity of revolution ($\dot{W}$) and rotational angular velocity ($n = 6.318\,11$) of the planet on its own axis as a function of time.

Van Hemelrijck and Vercheval, 1983) that from 9 days before to 9 days after the perihelion passage some fraction of the Sun is above the horizon; from day + 9 the Sun is completely visible. As a consequence of the existence of the thermal bulge, and owing to the fact that the Sun does not definitely set, it follows that after rising and receding the Sun rises again without disappearing completely (Figure 3). The maximum value of the instantaneous insolation for $e = 0.205\,63$ amounts to about 250 cal cm^{-2}(planetary day)$^{-1}$ at day-4; the minimum value, obtained symmetrically with respect to the perihelion, reaches slightly 15 cal cm^{-2}(planetary day)$^{-1}$. It is also interesting to note that the 18 days spend by the Sun to rise (or set) completely, correspond to roughly 20% of an orbital period ($T_0 = \sim 88$ Earth days).

As mentioned above, a striking difference exists for $e = 0.24$. Figure 3 reveals that, taking into account the finite angular size of the Sun's disk, the upper limb of the Sun breaks the horizon at day-13, whereas the lower limb disappears very shortly (day + 1) after the perihelion passage. The Sun temporarily sets, then rises again. For this configuration it is shown that the relatively short period of weak insolation (14 days) is followed (or preceded on the next orbit) by a time interval of complete darkness of approximately 11 days. Concerning more particularly the peak insolation of the thermal bulge, the sensitivity of I to changes in e is evident from Figure 3. Indeed, it can be seen that

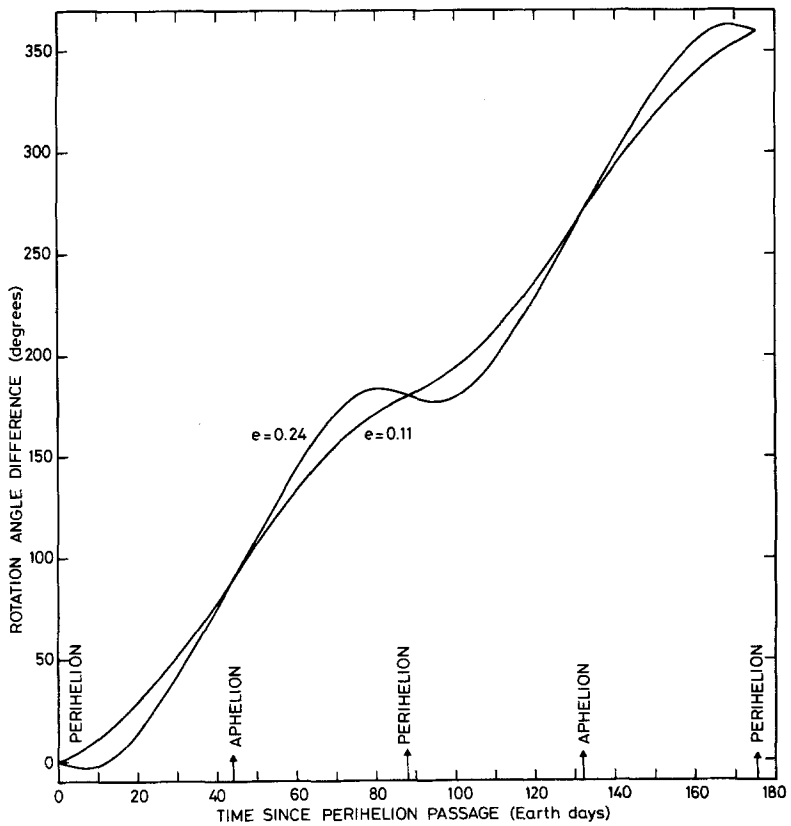

Fig. 5. Rotation angle differences ($nt - W$) for Mercury as a function of time.

the instantaneous insolation exhibits a sixfold [from 250 to 1500 cal cm^{-2}(planetary day)$^{-1}$] increase in going from the current value of e to the theoretical maximum one. For completeness, it has to be said that the critical value of e past which the Sun shortly sets after perihelion is near 0.213 (Van Hemelrijck and Vercheval, 1983).

4. The Daily Insolation

We also have investigated the daily insolation I_D as a function of the longitude difference $\Delta\lambda$ by application of expression (10). The integration limits t_1 and t_2 have been determined from relation (11) and (12) and from Figure 5 representing the variability of the function $f(t) = nt - W(t)$ over a time period equal to one Mercurian solar day and where $W(t)$ is given by formula (4). It has to be noticed that t_1 and t_2 corresponding to $e = 0.205\,63$ are taken from Van Hemelrijck and Vercheval (1981).

The distribution of the diurnal insolation, on the equator and for the three eccentricities studied in this paper, as a function of the longitude difference between the meridian

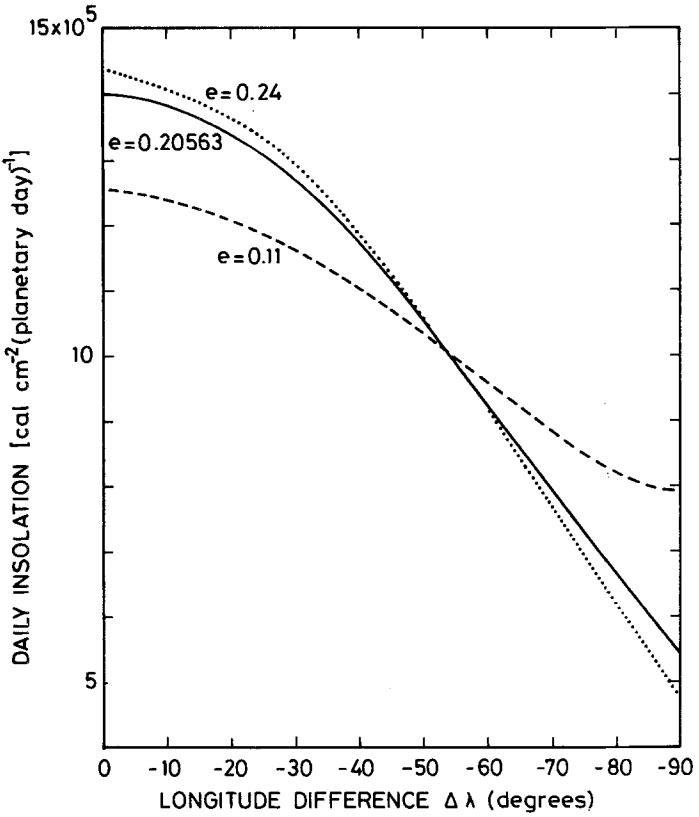

Fig. 6. Daily insolation at the top of Mercury as a function of the longitude difference $\Delta\lambda$. The curves correspond to the equator.

of a surface element and the meridian crossing the line of apsides at the perihelion passage of Mercury is plotted in Figure 6.

From an analysis of this Figure it may be concluded that the maximum daily insolation attained by a so-called hot pole ($\Delta\lambda = 0$) is about 1.25×10^6 ($e = 0.11$), 1.40×10^6 ($e = 0.205\,63$) and 1.45×10^6 ($e = 0.24$) cal cm^{-2}(planetary day)$^{-1}$. The minimum values occur at a warm pole ($\Delta\lambda = -90°$) and amount, respectively, to 7.95×10^5, 5.50×10^5 and 4.80×10^5 cal cm^{-2} (planetary day)$^{-1}$. It follows that the diurnal insolation decreases by nearly a factor of 1.6, 2.5, and 3.0 as the longitude difference increases from 0 to 90°. Furthermore, it is particularly evident from Figure 6 that the critical longitude difference past which the daily insolation at small eccentricities exceeds the one at large eccentricities is of the order of 55°.

5. Summary and Conclusions

In the preceding sections emphasis is placed on the influence of orbital eccentricity variations on the instantaneous and daily insolation on the planet Mercury.

The main results of this short study may be summarized as follows:

(a) At the hot pole of Mercury, the maximum percent difference in the instantaneous insolation in going from the minimum to the maximum value of the orbital eccentricity amounts to about 25% at the first and the third perihelion passage of the planet.

(b) At the warm pole, the percentage differences in the instantaneous insolation are significantly higher, with a minimum value of approximately 35% at aphelion.

(c) Taking into account the finite angular size of the Sun, especially at the warm pole, we find that there exist two permanent thermal bulges on opposite sides of the Mercurian surface that alternately face the Sun at every perihelion passage for eccentricities larger than about 0.194.

(d) For $0.194 < e < 0.213$ and at the warm pole the Sun rises, recedes, then rises again without disappearing completely.

(e) For $e > 0.213$ the Sun rises, temporarily sets, then rises again.

(f) The daily insolation on the equator decreases by nearly a factor of 1.6 (for $e = 0.11$) and 3.0 ($e = 0.24$) as the longitude difference ranges from 0 to 90°.

(g) As eccentricity increases, the daily insolation at the hot pole increases but conversely decreases at the warm pole. The longitude difference for which I_D is practically independent upon the orbital eccentricity is of the order of 55°.

In conclusion, we believe that long-term changes in the instantaneous and daily insolations on Mercury caused by variations of the Mercurian orbit have to be taken into account in order to better understand some aspects of the past and the present weather and climate on Mercury.

Acknowledgements

We would like to thank J. Schmitz and F. Vandreck for the realisation of the illustrations. We are also grateful to L. Vastenaekel for typing the manuscript.

References

Brouwer, D. and van Woerkom, A. J. J.: 1950, *Astron. Pap. Amer. Ephemeris Naut. Alm.* **13**, 81.
Cohen, C. J., Hubbard, E. C., and Oesterwinter, C.: 1973, *Celest. Mech.* 7, 438.
Landau, R.: 1975, *Icarus* **26**, 243.
Landau, R.: 1982, *Icarus* **52**, 202.
Levine, J. S., Kraemer, D. R., and Kuhn, W. R.: 1977, *Icarus* **31**, 136.
Liu, H.-S.: 1968, *Science* **159**, 306.
Morrison, D.: 1970, *Space Sci. Rev.* **11**, 271.
Soter, S. and Ulrichs, J.: 1967, *Nature* **214**, 1315.
Turner, L. E.: 1978, *Amer. J. Phys.* **46**, 475.
Van Flandern, T. C. and Harrington, R. S.: 1976, *Icarus* **28**, 435.
Van Hemelrijck, E.: 1982a, *Icarus* **51**, 39.
Van Hemelrijck, E.: 1982b, 'The Oblateness Effect on the Solar Radiation Incident at the Top of the Atmosphere of Mars', in *Proceedings of the Workshop on the Planet Mars*, Leeds, 1982, ESA special publication, SP-185, 59–63.
Van Hemelrijck, E.: 1982c, *Icarus* **52**, 560.
Van Hemelrijck, E.: 1982d, *Bull. Acad. R. Bel., Cl. Sci.* **68**, 675.

Van Hemelrijck, E.: 1983a, *Solar Energy* **31**, 223.
Van Hemelrijck, E.: 1983b, *The Moon and the Planets* **28**, 125.
Van Hemelrijck, E. and Vercheval, J.: 1981, *Icarus* **48**, 167.
Van Hemelrijck, E. and Vercheval, J.: 1983, 'A Comment on the Insolation at the warm Pole of Mercury', *Icarus* (submitted).
Vorob'yev, V. I. and Monin, A. S.: 1975, *Atmos. Ocean Phys.* 11, 557.
Ward, W. R.: 1974, *J. Geophys. Res.* **79**, 3375.
Ward, W. R., Colombo, G., and Franklin, F. A.: 1976, *Icarus* **28**, 441.
Wilson, R. C.: 1982, *J. Geophys. Res.* 87, 4319.